

## Star Forming Regions in Cassiopeia

Mária Kun

*Konkoly Observatory, H-1525 Budapest, P.O. Box 67, Hungary*

**Abstract.** This chapter describes the Galactic star forming regions in the constellation Cassiopeia, in the Galactic coordinate range  $120^\circ \lesssim l \lesssim 130^\circ$ ,  $-5^\circ \lesssim b \lesssim 15^\circ$ . At  $|b| > 10^\circ$  the nearby clouds L 1333 and L 1340 are found in this region. The local arm of the Galaxy in Cassiopeia contains only a few star forming regions, smaller and less active than the OB associations of the neighboring Cepheus. Five members of this system, LkH $\alpha$  198 and its environment, L 1287, L 1293, L 1302/NGC 255, and S 187 are discussed. Several more distant OB associations and giant star forming regions in Cassiopeia are associated with the Perseus arm at 2.0–3.0 kpc. Among these, the Herbig Be star MWC 1080 is discussed in this chapter.

### 1. Overview

The large-scale distribution of the dark clouds in Cassiopeia, adopted from the Atlas and Catalog of Dark Clouds (Dobashi et al. 2005), is displayed in Fig. 1. The most prominent clouds and young stellar objects are marked.

The high Galactic latitude region of the constellation Cassiopeia contains a few nearby star forming molecular clouds. The nearest cloud is Lynds 1333 at  $(l, b) = (129^\circ, +15^\circ)$  and at  $d \approx 180$  pc, associated with a few low-mass pre-main sequence stars. Lynds 1340, a region of intermediate and low mass star formation, can be found at  $(l, b) = (130^\circ, +11^\circ.5)$  at  $d \approx 600$  pc. Towards lower latitudes, the cloud complex L 1355/L 1358 is located at  $(l, b) \sim (133^\circ.5, +8^\circ.6)$ . This complex is illuminated by a loose group of B and A stars and the classical Cepheid SU Cas (Turner & Evans 1984). The average distance of these stars, determined by Turner & Evans (1984) is  $d = 258 \pm 3$  pc. No star formation has been observed in these clouds. The starless cores of L 1355 and L 1358 have been targets of several studies aimed at observing initial conditions of low-mass star formation and protostellar infall (Lee, Myers, & Tafalla 1999, 2001; Park, Lee, & Myers 2004).

Star forming regions at various distances can be found at latitudes ( $|b| < 10^\circ$ ). The catalog of CO clouds associated with IRAS point sources, published by Kerton & Brunt (2003), contains numerous likely star forming regions which deserve follow-up studies. L 1265, L 1287, and S 187, located between 600–1000 pc, are associated with the Orion arm of our Galaxy. The most distant star forming regions, associated with the Perseus arm, include several OB associations (e.g. Humphreys 1978; Garmany & Stencel 1992) located between 1.8–2.8 kpc, and the Herbig Be star MWC 1080, one of the best studied members of this class of objects. The most prominent member of this system, the giant star forming complex W3/W4/W5 is discussed in the chapter by Megeath et al. The regions discussed in the present chapter are listed in Table 1.

## 2. Lynds 1333

Lynds 1333 is a small dark cloud of opacity class 6 at  $(l, b) = (128^\circ 88', +13^\circ 71')$  (Lynds 1962). Obayashi et al. (1998) derived a distance of  $180 \pm 20$  pc using a Wolf diagram, and mapped the cloud in  $^{13}\text{CO}$  and  $\text{C}^{18}\text{O}$ . According to the available data, the L 1333 dark cloud itself is starless, and has been included in several studies of starless cores (e.g. Lee et al. 1999, 2001, 2004).  $^{13}\text{CO}$  and  $\text{C}^{18}\text{O}$  observations by Obayashi et al. (1998) have shown this dark cloud to be part of a long (some 30 pc), filamentary cloud complex ( $126^\circ \leq l \leq 133^\circ$ ,  $+13^\circ \leq b \leq +15^\circ$ ). They refer to this molecular com-

Table 1. Star-forming molecular clouds in Cassiopeia

Dark Cloud <sup>a</sup>	CO cloud <sup>b</sup>	d (pc)	Associated YSO
L 1238	111.7+00.0	2200	MWC 1080
L 1265	117.8−03.6	600	LkH $\alpha$ 198
...	120.1+03.0 <sup>c</sup>	850	IRAS 00213+6530, IRAS 00259+6510
L 1287, TDS463	121.3+00.6	850	RNO 1, IRAS 00338+6312
L 1293	121.7+00.2	850	IRAS 00379+6248
L 1302	122.0−01.1	600	BD +61° 154, LkH $\alpha$ 201
L 1317	126.6−00.6	800	S 187
L 1333	129.0+13.8	180	IRAS 02086+7600
L 1340	131.1+11.6	600	RNO 7,8,9

<sup>a</sup> Lynds (1962); Taylor, Dickman, & Scoville (1987);

<sup>b</sup> Yonekura et al. (1997);

<sup>c</sup> This cloud lies within the region studied in this chapter, but, as it is associated with Cep OB 4 in the literature, it is discussed in the Cepheus chapter.

plex as the *L1333 molecular cloud* (Fig. 2). Star formation in the L 1333 molecular cloud has been indicated by the presence of the protostellar-like (Class I SED) source IRAS 02086+7600 and by three other IRAS sources coinciding with H $\alpha$  emission stars. Comparison of the properties of dense C<sup>18</sup>O cores of L 1333 with those of other nearby star forming clouds (Taurus, Ophiuchus, Lupus, and Chamaeleon) suggests that L 1333 is among the smallest known star forming molecular cloud complexes (Onishi et al. 1999; Tachihara et al. 2000, 2002). It represents an extreme environment of star formation, where a few low-mass stars are being formed in a small, filamentary cloud complex.

The total mass of <sup>13</sup>CO molecular clouds shown in Fig. 2 is estimated to be about 720  $M_{\odot}$ . Thirteen C<sup>18</sup>O cores, which are characterized by mean mass of 9  $M_{\odot}$  and mean density of  $1.4 \times 10^4 \text{ cm}^{-3}$ , are embedded in the <sup>13</sup>CO cloud.

Eighteen H $\alpha$  emission line stars have been detected within or near the <sup>13</sup>CO clouds on objective prism plates. Spectroscopic follow-up observations confirmed the pre-main sequence nature of only three of them. One of the three, OKS98 H $\alpha$  6, proved to be a visual double with two T Tauri type components, separated by 1''8. Table 2 shows the IRAS and 2MASS data for these objects, as well as spectral types and optical photometric results (Kun et al. 2006). Their distribution with respect to the molecular cloud is displayed in Fig. 2. The source IRAS 02086+7600 is associated with a C<sup>18</sup>O core and exhibits a Class I type infrared spectrum, yet coincides with a faint visible star.

There are several weak-line T Tauri stars in the cloudless region between L 1333 and the high-longitude edge of the Cepheus flare ( $116^{\circ} < l < 124^{\circ}$ ,  $b \sim 17^{\circ}$ , found by Tachihara et al. (2005)). Their relation to the cloud complex is unknown.

Olano et al. (2006) studied the space distribution and kinematics of the interstellar matter in the Cepheus flare and in the neighboring Cassiopeia clouds, using the Leiden–Dwingeloo HI data and the Columbia Survey CO data. They found that the broad and often double-peaked spectral line profiles suggest that the Cepheus Flare and Cassiopeia clouds form a big expanding shell that encloses an old supernova remnant. Assuming a distance of 300 pc for the center of the shell they derived a radius of approximately 50 pc, expansion velocity of 4 km s<sup>−1</sup>, and HI mass of  $1.3 \times 10^4 M_{\odot}$  for the Cepheus

Flare Shell. L 1333 probably lies on the approaching side of the Cepheus Flare Shell, whose approximate position is plotted in Fig. 1.

Table 2. Low-mass pre-main sequence stars in L 1333

IRAS 2MASS OKS98 H $\alpha$	$F_{12}$ Sp.	$F_{25}$ $J$ $V$	$F_{60}$ $H$ $R_C$	$F_{100}$ $K_s$ $I_C$
IRAS 02086+7600	0.25	2.68	7.41	10.49
02134360+7615059		13.715	12.254	11.193
...	...	19.71	17.81	16.47
IRAS F02084+7605	0.12	0.14	<0.29	<7.18
02133179+7619127		10.648	9.725	9.317
OKS98 H $\alpha$ 5	M0.5IV	15.49	14.12	12.76
IRAS 02103+7621	0.51	0.58	0.33:	<1.93
02152532+7635196		10.222	9.342	8.701
OKS98 H $\alpha$ 6 N	K7V	13.19	12.57	11.78
OKS98 H $\alpha$ 6 S	M2IV	...	15.73	14.10
IRAS 02368+7453	0.44	0.89	0.89	3.21
02420054+7505473		10.920	9.654	8.963
OKS98 H $\alpha$ 16	K5III	17.42	15.57	13.52

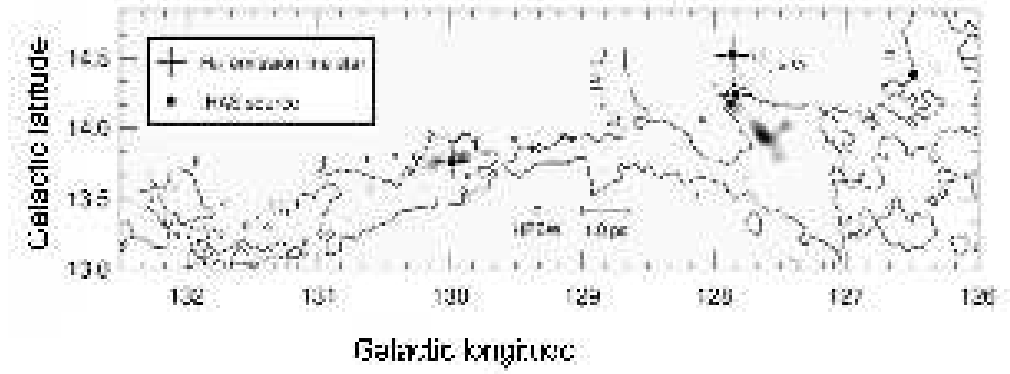


Figure 2. Integrated intensity map of the  $^{13}\text{CO}$  (contour) and  $\text{C}^{18}\text{O}$  (gray scale) and the positions of the bona fide YSOs in the L 1333 cloud complex. Crosses mark the OKS H $\alpha$  stars (Obayashi et al. 1998), and dots are IRAS point sources.

### 3. Lynds 1340

Lynds 1340 is a dark cloud of opacity class 5 at  $(l, b) = (130^\circ, +11^\circ)$  (Lynds 1962). It is associated with the reflection nebula DG 9 (Dorschner & Gürtler 1964), illuminated by B and A-type stars. The small nebulosities RNO 7, 8, and 9 (Cohen 1980), associated with the cloud, are probably signposts of recent star formation. The basic properties of the cloud were studied by Kun et al. (1994). They presented  $^{13}\text{CO}$  and  $\text{C}^{18}\text{O}$  maps of the cloud, and obtained a distance of  $600 \pm 60$  pc by averaging the results obtained

from a Wolf diagram, as well as the spectral classification and *UBV* photometry of the stars illuminating DG 9. They also provided a list of candidate young stellar objects, selected from the IRAS catalogs and  $H\alpha$  emission stars identified on objective prism Schmidt plates. Yonekura et al. (1997) found that L 1340 contains some  $1300 M_{\odot}$  of molecular mass.

The distribution of  $^{13}\text{CO}$  has revealed three clumps within the cloud, denoted as L 1340 A, B, and C by Kun et al. (1994). Each clump is associated with massive  $\text{C}^{18}\text{O}$  cores, and with a number of IRAS point sources and  $H\alpha$  emission stars.

The densest regions of L 1340 were mapped in the (1,1) and (2,2) inversion transition lines of ammonia (Kun, Wouterloot, & Tóth 2003). The ammonia survey has revealed 10 dense cores, occupying some 7 % of the mapped area. Their total mass is  $\sim 80 M_{\odot}$ , about 6 % of the mass traced by  $\text{C}^{18}\text{O}$ .

Kumar, Anandarao, & Yu (2002) performed a near infrared imaging survey and search for Herbig–Haro objects in L 1340. They established that RNO 7 is a small embedded cluster consisting of some 26 members, and identified three Herbig–Haro flows in L 1340 A. The source of HH 487 is probably IRAS 02224+7227, coinciding in position with an M type weak-line T Tauri star (Kun et al. 2006). HH 488 originates from RNO 7, and HH 489 from the Class I source IRAS 02250+7230.

Magakian et al. (2003) identified further HH objects, HH 671 and HH 672, originating from RNO 7. They detected 14  $H\alpha$  emission stars in the region of RNO 7. Table 4 lists the IRAS point sources and  $H\alpha$  emission stars selected as candidate YSOs by Kun et al. (1994) and Magakian et al. (2003), and Table 3 lists the known HH objects and sources in L 1340. Figure 3 shows the surface distribution of  $^{13}\text{CO}$ ,  $\text{C}^{18}\text{O}$ , and visual extinction, and positions of ammonia cores, IRAS point sources, and RNOs in L 1340, adopted from Kun et al. (2003). Figure 4, adopted from Magakian et al. (2003), is the finding chart of the  $H\alpha$  emission stars near RNO 7.

O’Linger et al. (2007) mapped L 1340 B at 450 and  $800\mu\text{m}$  using SCUBA on JCMT. They discovered 25 submillimeter sources. By mapping the region in the J=3-2 transition of CO, they discovered outflows around several sources. The submm sources are listed in Table 5. There are several Class 0 protostars among them. O’Linger et al. (2007) conclude that these sources represent a second generation of stars born in the cloud, and their formation might have been triggered by the Herbig Be star KOS94 R3b, located in the same cloud.

#### 4. Star Forming Regions at $|b| < 10^\circ$

The pre-main sequence stars in Cassiopeia at  $|b| < 10^\circ$  are listed in Table 6, and the outflow-driving objects are shown in Table 7.

##### 4.1. LkH $\alpha$ 198 and its Environment in Lynds 1265

The pre-main sequence star LkH $\alpha$  198 (V633 Cas, HBC 3), associated with the dark cloud L 1265, was first identified by Herbig (1960). Cohen & Kuhl (1979) classified its spectral type as B3, Hillenbrand et al. (1992) as A5, and Hernández et al. (2004) as B9. Chavarría-K. (1985) discovered the photometric variability, in particular, flare activity of LkH $\alpha$  198. He derived a distance of 600 pc and a luminosity of  $160 L_{\odot}$  for LkH $\alpha$  198, and established that the star is some 2.5 mag above the main sequence. Its eventual spectral type on the main sequence is expected to be about B3. V376 Cas,

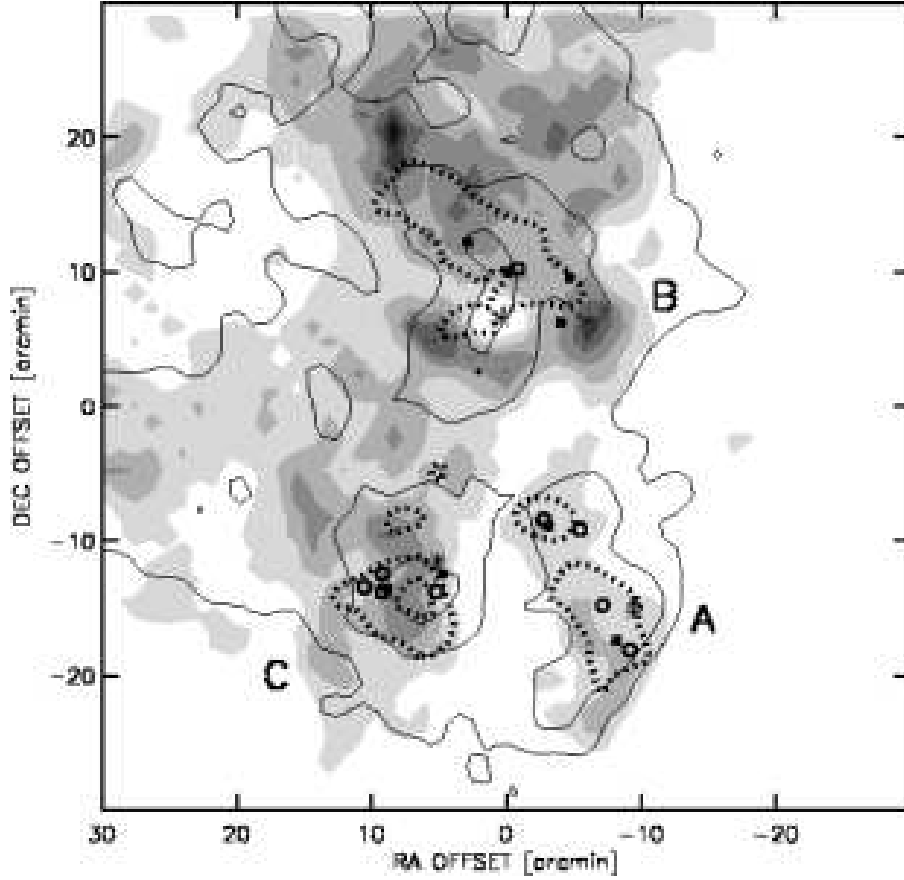


Figure 3.  $^{13}\text{CO}$  (solid contours) and  $\text{C}^{18}\text{O}$  (dotted contours) integrated intensity overlaid on the optical extinction map (shading) of L1340 constructed from star counts on the DSS. Coordinate offsets are given in arcmin with respect to  $\text{RA}(2000)=2^{\text{h}}29^{\text{m}}42^{\text{s}}$  and  $\text{Dec}(2000)=+72^{\circ}43'22''$ . The lowest contour of  $^{13}\text{CO}$  is at  $1.0 \text{ K km s}^{-1}$ , and the increment is  $1.5 \text{ K km s}^{-1}$ . The  $\text{C}^{18}\text{O}$  contours displayed are  $0.45$  and  $0.75 \text{ K km s}^{-1}$ . Both the lightest shade and the increment is  $1 \text{ mag}$ . The  $A_V$  values displayed are corrected for the foreground extinction. Open circles indicate the ammonia cores, which probably represent the regions of highest volume densities. Dots are optically invisible IRAS point sources, and asterisks show the positions of the RNOs.

another Herbig Be star, is located  $37''$  north of  $\text{LkH}\alpha 198$  within the same cloud. Lagage et al. (1993) imaged the region around  $\text{LkH}\alpha 198$  at  $10 \mu\text{m}$ , and discovered a deeply embedded companion  $6''$  north of the star, which they suggest to be responsible for most of the far-infrared emission in the region. The mid-infrared companion was also detected in the near-infrared by Li et al. (1994) and Leinert et al. (1997). The projected separation of the binary is  $3300 \text{ AU}$ . The estimated luminosity of the companion is  $100 L_{\odot}$ , thus it could be a third Herbig Ae/Be star in the system.

Cantó et al. (1984) and Leveault (1988) found a large CO outflow from the system. Strom et al. (1986) discovered an HH object, HH 161, south-east of  $\text{LkH}\alpha 198$ . Corcoran et al. (1995) found two further HH flows, HH 162, associated with V376 Cas,

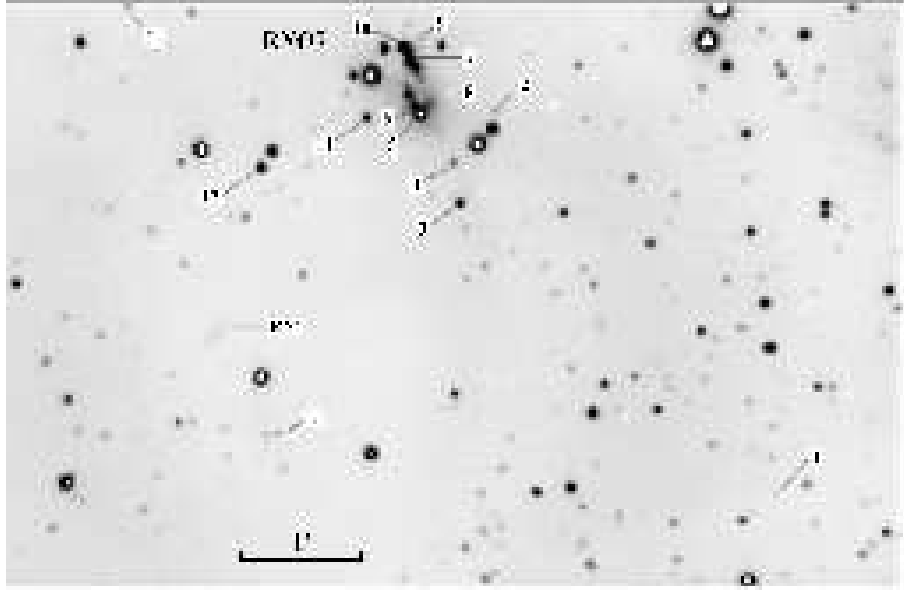


Figure 4.  $H\alpha$  emission stars and a reflection nebula (RN 1) detected by Magakian et al. (2003) near RNO 7.

Table 3. Herbig-Haro objects in L 1340

Object	RA(J2000)	Dec(J2000)	Comments	Source	Ref.
HH 487A	02 26 19.0	72 34 42	Bow shocks	IRAS 02224+7227	1
HH 488 S1	02 28 00.3	72 35 58	Source plus jet		1
HH 488 S2	02 28 00.0	72 35 58	Source plus jet		1
HH 671A	02 28 16.1	72 37 45			2
HH 671B	02 28 09.2	72 36 28			2
HH 488A	02 28 22.5	72 34 56	Flow 1		1,2
HH 488B	02 28 30.6	72 34 37			2
HH 488C	02 28 40.0	72 34 16	Flow 1		1
HH 488D	02 28 44.0	72 35 37	Flow 2		1
HH 488E	02 28 38.6	72 34 30			2
HH 489A	02 29 37.7	72 44 50	North knot	IRAS 02250+7230	1
HH 672	02 28 53.2	72 36 13			2

References: 1 – Kumar et al. (2002); 2 – Magakian et al. (2003).

and HH 164. They identified LkH $\alpha$  198 as the driving source of HH 164, and the embedded companion, LkH $\alpha$  198 B, as the source of HH 161. Aspin & Reipurth (2000) by optical imaging discovered a bright bow shock, HH 461, along the axis defined by the previously known HH 164 jet.

Sandell & Weintraub (1994) presented submillimeter and millimeter line and continuum observations of the region around LkH $\alpha$  198 and V376 Cas. The continuum data revealed the presence of a very cool object, LkH $\alpha$  198 MM, located 19'' northwest of LkH $\alpha$  198. LkH $\alpha$  198 MM is not visible in the near-infrared. The CO maps suggest that the mm-source, rather than LkH $\alpha$  198 or its infrared companion LkH $\alpha$  198 B, may drive the large CO outflow seen in this cloud, or that both the stars and the millimeter

Table 4. IRAS sources and H $\alpha$  emission stars in L 1340

Names	2MASS/RA,DEC	J	H	K <sub>s</sub>	Type*
L 1340 A					
IRAS 02224+7227, HH 487 S	02270555+7241167	9.901	9.084	8.579	WTTS
MMN03 H $\alpha$ 1	02273240+7234040				
HH 488 S2	02275976+7235561	16.763	16.101	15.348	
HH 488 S1	02280134+7236104	16.202	15.372	15.199	
MMN03 H $\alpha$ 2	02280700+7237345	14.873	13.415	12.600	
MMN03 H $\alpha$ 3	02281182+7236447	13.110	11.695	10.784	
MMN03 H $\alpha$ 4	02281259+7237067	15.158	14.027	13.536	
IRAS 02236+7224, KOS94 H $\alpha$ 1, MMN03 H $\alpha$ 5	02281661+7237328	11.715	10.406	9.247	
MMN03 H $\alpha$ 6	02281748+7237384	14.070	12.893	12.278	
MMN03 H $\alpha$ 7	02281782+7238009	12.298	10.977	9.903	
MMN03 H $\alpha$ 8	02281840+7237479	15.077	13.878	13.196	
KOS94 H $\alpha$ 2b, MMN03 H $\alpha$ 9	02281877+7238091	12.397:	12.223	11.715	
KOS94 H $\alpha$ 2, MMN03 H $\alpha$ 10	02281818+7238069	12.194:	11.385	10.451	CTTS
IRAS 02238+7222	02283280+7235270				
MMN03 H $\alpha$ 11	02282357+7237317	13.596	12.499	12.020	
MMN03 H $\alpha$ 12	02283719+7237061	13.085	12.197	11.820	
MMN03 H $\alpha$ 13	02283760+7234430				
KOS94 H $\alpha$ 5	02285180+7239143	12.933	11.989	11.326	CTTS
MMN03 H $\alpha$ 14	02285420+7238352	14.538	13.493	12.834	
IRAS 02250+7230, HH 489 S	02294309+7243597	16.028	14.898	13.914	
L 1340 B					
IRAS 02232+7250, L1340 B smm 1	02280003+7304073	14.463	13.101	12.542	
IRAS 02232+7250, L1340 B smm 1	02280074+7304154	15.493	13.476	11.895	
KOS94 R3b	02292062+7304514	11.771	11.702	11.576	HBe
KOS94 H $\alpha$ 9, L1340B smm 8	02292109+7258120	12.160	11.428	11.003	CTTS
IRAS F02246+7248, L1340B smm 10	02292330+7302220				
IRAS 02247+7245, L1340B smm 11	02292910+7259040				
KOS94 H $\alpha$ 4	02293037+7311429	12.821	11.523	10.658	CTTS
IRAS 02256+7249	02302610+7302460				
IRAS 02259+7246, RNO 8	02303247+7259177	13.628	12.229	10.899	CTTS
RNO 8 s1	02303681+7259566	13.309	12.511	12.134	CTTS
RNO 8 s2	02303911+7259572	12.026	10.537	9.403	CTTS
IRAS 02263+7251	02310640+7304580				
L 1340 C					
IRAS 02267+7226	02312688+7240191	15.114:	13.757	12.699	
IRAS 02267+7226	02312871+7240158	18.501:	16.190	14.765	
RNO 9 s2	02313994+7241575	13.826	12.658	12.098	CTTS
RNO 9	02314031+7241419	11.499	10.582	9.831	F3IVe
IRAS 02276+7225	02322210+7239020				
IRAS F02277+7226	02322888+7240561	15.589	14.948	14.726	
IRAS F02279+7225, KOS94 H $\alpha$ 10	02323897+7239038	12.291	11.081	10.209	
KOS94 H $\alpha$ 11	02330153+7243269	16.494	14.675	12.921	
KOS94 H $\alpha$ 13	02350799+7251034	12.936	11.950	11.218	CTTS

KOS94 H $\alpha$ : H $\alpha$  emission stars listed in Kun et al. (1994);

MMN03 H $\alpha$ : H $\alpha$  emission stars listed in Magakian et al. (2003).

\*Kun et al., in preparation.



Figure 6. LkH $\alpha$ 198 [SII]: Mosaic of the entire outflow around LkH $\alpha$  198, adopted from McGroarty et al. (2004). North is to the left and west to the top in this figure.

Table 5. Submillimeter sources in L 1340 B from O’Linger et al. (2007)

Name	RA(J2000)	Dec.(J2000)	remarks
L1340 B smm 1	02 27 55.3	73 04 15	IRAS F02232+7250?, multiple (5 peaks)
L1340 B smm 2	02 28 07.1	72 59 08	multiple (4 peaks)
L1340 B smm 3	02 28 08.9	73 04 07	multiple (3 peaks)
L1340 B smm 4	02 28 14.3	73 05 29	multiple (2 peaks)
L1340 B smm 5	02 28 19.7	73 05 11	single
L1340 B smm 6	02 28 52.6	73 01 17	multiple (3 peaks) no IRAS, no outflow, prestellar
L1340 B smm 7	02 29 05.4	73 01 12	single, no outflow, prestellar
L1340 B smm 8	02 29 18.4	72 58 12	single, no outflow, 2MASS
L1340 B smm 9	02 29 20.3	73 01 21	probably outflow, no IRAS
L1340 B smm 10	02 29 20.8	73 02 23	F02246+7248, 02291961+7302237, 3 peaks, Class 0, Class I
L1340 B smm 11	02 29 32.0	72 59 17	02248+7245, prob. Class 0
L1340 B smm 12	02 29 56.4	73 02 20	F02252+7248, outflow, bright, Class 0
L1340 B smm 13	02 29 59.5	73 02 53	outflow, no IRAS, no 2MASS, Class 0
L1340 B smm 14	02 30 04.3	73 02 50	no IRAS, no 2MASS, prob. Class 0
L1340 B smm 15	02 30 08.4	73 02 53	no IRAS, no 2MASS, prob. Class 0
L1340 B smm 16	02 30 18.7	73 02 48	3 peaks, prob. Class 0
L1340 B smm 17	02 30 22.7	73 05 03	no IRAS, no 2MASS, Class 0 or prestellar
L1340 B smm 18	02 30 34.9	73 00 17	3 peaks, cluster of at least 6 2MASS sources
L1340 B smm 19	02 30 35.3	73 03 42	at least 3 peaks, outflow, Class 0+Class I
L1340 B smm 20	02 30 41.6	73 01 59	no IRAS, no 2MASS, prob. Class 0
L1340 B smm 21	02 30 42.3	73 03 10	outflow, faint 2MASS, prob. Class 0
L1340 B smm 22	02 30 43.8	73 04 24	prob. Class 0 or Class I
L1340 B smm 23	02 30 45.0	73 01 39	outflow, no IRAS, no 2MASS, Class 0
L1340 B smm 24	02 30 55.1	72 58 07	no IRAS, no outflow
L1340 B smm 25	02 31 02.3	72 58 09	outflow, no IRAS, no 2MASS, Class 0

source drive outflows which are roughly parallel to each other. In addition V376 Cas appears to power a small bipolar CO outflow.

Butner & Natta (1995) modeled the extended far-infrared emission, measured by KAO, from the system, and established that the source of the emission is the optical star LkH $\alpha$  198, and not its infrared companion. High resolution interferometry toward LkH $\alpha$  198 and the surrounding region by di Francesco et al. (1997) at 2.7 mm failed to detect LkH $\alpha$  198, but LkH $\alpha$  198 MM was detected and resolved. Hajjar & Bastien (2000) revisited the probable protostellar object LkH $\alpha$  198 MM northwest of LkH $\alpha$  198. They found it to be the main source of emission in the region at millimeter wavelengths and probably the major contributor to the submillimeter radiation down to 100  $\mu$ m, and the most likely source of the large-scale CO outflow.

The stars are embedded in a reflection nebula (see the left panel of Fig. 5), which was also detected in the near infrared by Testi et al. (1998). The NIR nebula prevented Testi et al. from detecting a possible group of low-mass stars, usually present around Herbig Be stars.

Fukagawa et al. (2002) carried out high-resolution near-infrared imaging of LkH $\alpha$  198 using the Coronagraphic Imager with Adaptive Optics (CIAO) on the Subaru 8.2-m Telescope. The images resolve the infrared companion LkH $\alpha$  198 B and an associated parabolic reflection nebula, indicating that it is an outflow source. LkH $\alpha$  198 B exhibits

Table 6. Pre-main sequence stars in Cassiopeia located at  $|b| < 10^\circ$ 

Names	IRAS	RA(J2000)	Dec(J2000)	Type	Cloud	Ref.
HBC 317, MWC 1080	23152+6034	23 17 25.6	60 50 43	Cont.	L 1238	1
HBC 2, LkH $\alpha$ 197		00 10 36.4	58 50 05	K7	L 1265	1
HBC 3, LkH $\alpha$ 198	00087+5833	00 11 26.0	58 49 29	A	L 1265	1
HBC 325, V376 Cas		00 11 26.1	58 50 03	B5e	L 1265	1
HBC 329, VX Cas	00286+6142	00 31 30.7	61 58 51	A0e		1
RNO 1B, V710 Cas		00 36 46.3	63 28 54	F8IIe	L 1287	5,6
RNO 1C		00 36 46.8	63 28 58	FU Ori	L 1287	6
HBC 6, LkH $\alpha$ 200, V828 Cas		00 42 29.3	61 55 46	K1	L 1291	1
HBC 330, BD +61 $^\circ$ 154, MWC 419, V594 Cas, VDB 4	00403+6138	00 43 18.3	61 54 40	B8	L 1302	1
HBC 7, LkH $\alpha$ 201		00 43 25.3	61 38 23	B3e	L 1302	1
HBC 331, LkH $\alpha$ 203		00 44 27.4	62 10 46	K5	L 1302	1
HBC 332, LkH $\alpha$ 204		00 45 09.9	62 04 26	K8	L 1302	1
GLMP 9	00422+6131	00 45 09.9	61 47 57	T Tau	L 1302	4
HBC 333, LkH $\alpha$ 205		00 45 26.3	61 38 53	Cont.	L 1302	1
GLMP 11	00470+6130	00 50 04.0	61 47 05	T Tau	L 1302	4
S 187 H $\alpha$		01 20 15.2	61 33 08	Be	L 1317	2
SCP NIRS 1		01 23 18.2	61 47 40	T Tau	L 1317	3

*References:* 1 – Herbig & Bell (1988); 2 – Zavagno et al. (1994); 3 – Salas et al. (1998); 4 – García-Lario et al. (1997); 5 – Staude & Neckel (1991); 6 – Kenyon et al. (1993).

Table 7. Outflow driving sources in Cassiopeia at  $|b| < 10^\circ$ 

Object	IRAS	RA(J2000)	Dec(J2000)	Ref.
MWC 1080	23152+6034	23 17 25.6	60 50 43	1,2,3
LkH $\alpha$ 198	00087+5833	00 11 26.0	58 49 29	1,2
M 120.1+3.0	00213+6530	00 24 10.4	65 47 01	9
M 120.1+3.0	00259+6510	00 28 50.9	65 26 46	9
L 1287	00338+6312	00 36 47.5	63 29 02	4,5
L 1293	00379+6248	00 40 53.5	63 04 53	6
S 187 IRS		01 23 15.0	61 48 47	7
SCP NIRS 1		01 23 18.2	61 47 40	8

*References:* 1 – Cantó et al. (1984); 2 – Levreault (1988); 3 – Koo (1989); 4 – Yang et al. (1991); 5 – Snell et al. (1990); 6 – Yang (1990); 7 – Bally & Lada (1983); 8 – Salas et al. (1998); 9 – Yang et al. (1990).

near-infrared colors suggestive of a Class I-like source. Faint nebulae associated with outflow activity and a bright flattened envelope were also found around the primary.

McGroarty et al. (2004) discovered a 2 pc long optical outflow powered by LkH $\alpha$  198. They discovered new Herbig-Haro objects, HH 800, HH 801, HH 802, originating from the system. Fig. 6, adopted from McGroarty et al. (2004) shows all the HH objects around the LkH $\alpha$  198 system. Perrin et al. (2004) have used laser guide star adaptive optics and a near-infrared dual-channel imaging polarimeter to observe light scattered in the circumstellar environment of Herbig Ae/Be stars on scales of 100 to 300 astronomical units. They detected a strongly polarized, biconical nebula 10 arcsec (6000 AU) in diameter around LkH $\alpha$  198 and also observed a polarized jet-like fea-

ture associated with the deeply embedded source LkH $\alpha$  198-IR. Smith et al. (2005) detected a close optical companion of LkH $\alpha$  198, based on diffraction-limited bispectrum speckle interferometry observations (right panel of Fig. 5). The new object, LkH $\alpha$  198 A2 lies at a separation of approximately 60 mas, or 36 AU from the brighter component. The plane of its orbit appears to be significantly inclined to the plane of the circumprimary disk, as inferred from the orientation of the outflow.

Matthews et al. (2007) combined  $^{12}\text{CO}$  data from FCRAO with high resolution BIMA array data to achieve a naturally weighted synthesized beam of  $6.75'' \times 5.5''$  toward LkH $\alpha$  198. They found that the outflow around LkH $\alpha$  198 resolves into at least four outflows, none of which are centered on LkH $\alpha$  198-IR.

#### 4.2. L 1287

L 1287 (TDS 463) is a filamentary dark cloud, located at 850 pc from the Sun (Yang et al. 1991), and extending over 10 pc along the Galactic plane. Yang et al. (1991) mapped the cloud in  $^{13}\text{CO}$ ,  $\text{HCO}^+$ , and HCN lines. The total mass of the cloud was estimated to be some  $240 M_{\odot}$  from the  $^{13}\text{CO}$  observations. It contains at least four separate cores, aligned along the filament. The region of strongest CO emission, *L 1287 main core*, contains a mass of some  $13 M_{\odot}$ , according to the  $^{13}\text{CO}$  observations. The IRAS point source IRAS 00338+6312 is projected on the peak CO position of L 1287 (Fig. 7 left panel, adopted from Yang et al. 1991). An energetic bipolar molecular outflow has been detected around this source (Snell et al. 1990; Yang et al. 1991), and it is associated with  $\text{H}_2\text{O}$  (Henning et al. 1992; Fiebig 1995; Fiebig et al. 1996), OH (Wouterloot, Brand, & Fiegle 1993), as well as methanol (Slysh et al. 1999; Kalenskii, Promyslov & Winnberg 2007) maser emission.

Walker & Masheder (1997) presented  $\text{HCO}^+$  ( $J=1-0$ ) and CS ( $J=2-1$  and  $5-4$ ) data for the molecular cloud centred on IRAS 00338+6312. They found that the line profiles suggest a collapsing cloud with density and infall velocity increasing towards the centre as  $r^{-3/2}$  and  $r^{-1/2}$ , respectively, in accordance with the predictions by Shu (1977). Mookerjee et al. (1999) observed IRAS 00338+6312 using the two-band FIR photometer system at the Cassegrain focus of the TIFR 100 cm (f/8) balloon-borne telescope. An area of  $22' \times 7'$  centered on IRAS 00338+6312 was mapped in the FIR bands at  $143 \mu\text{m}$  and  $185 \mu\text{m}$ . The source was resolved at both wavelengths.

L 1287 harbors the nebulous young star RNO 1 (F5e, Cohen 1980). Staude & Neckel (1991) discovered a further young stellar object located at  $50''$  south-west of RNO 1 ( $0.2 \text{ pc}$  at a distance of  $800 \text{ pc}$ ) which they called RNO 1B. Based on optical spectroscopic observations they have shown that RNO 1B is a FU Orionis type star. Further faint, probably deeply embedded stars can be identified in their *I*-band image near RNO 1 (right panel of Fig. 7). Near-infrared spectroscopic observations by Kenyon et al. (1993) confirmed the FUor nature of RNO 1B, and have shown that RNO 1C, located at  $6''$  from RNO 1B, is also a FUor. Kenyon et al. (1993) suggest that the binary system RNO 1B/RNO 1C is the driving source of the molecular outflow.

IRAS 00338+6312 is  $5''$  and  $11''$  from RNO 1C and RNO 1B, respectively. A number of observations support that the catalog coordinates of IRAS 00338 +6312 accurately mark the location of a deeply embedded YSO, distinct from the FUors. Using polarimetric imaging, Weintraub & Kastner (1993) found an embedded protostar that they suggested was the star driving the molecular outflow, since the position of the protostar was closer than either RNO 1B or 1C to the position of the IRAS source. VLA observations by Anglada et al. (1994) revealed four  $3.6 \text{ cm}$  sources within  $30''$  of the

IRAS position, all four of which are possibly PMS objects embedded in the L 1287 cloud core. The position of the strongest VLA source, VLA 3, coincides within the errors with the position of the protostar found by Weintraub & Kastner, while a second of the VLA sources, VLA 1, appears to coincide with the position of RNO 1C. McMuldroy et al. (1995) using the OVRO millimeter array detected a millimeter continuum source at both 3.1 and 2.6 mm, whose position coincides within the errors with that of RNO 1C. Neither RNO 1B nor VLA 3 were detected in the millimeter continuum, a result which would argue for RNO 1C being the source driving the outflow. The 850 and 450  $\mu\text{m}$  SCUBA maps obtained by Sandell & Weintraub (2001) show a strong elliptical dust source (RNO 1 SM 1) centered very close to the position of RNO 1C. The long axis of RNO 1 SM 1 ( $\sim +18^\circ$ ) is roughly orthogonal to the position angle of the CO outflow ( $\sim -50^\circ$ ). In addition to the large central source, the maps reveal a large region of emission surrounding RNO 1 SM 1 and a ridge of emission extending to the southeast. In the high-resolution 450  $\mu\text{m}$  image, an extension from RNO 1 SM 1 can be seen in the direction of the protostellar source VLA 3, supporting that that VLA 3 also is associated with dust emission. Along the southeast ridge, the SCUBA maps show the presence of two additional submillimeter sources, RNO 1 SM 2 and RNO 1 SM 3, both of which are securely detected at 1.3 mm and 850  $\mu\text{m}$ . No optical, infrared or IRAS counterparts are known at the positions of either RNO 1 SM 2 or RNO 1 SM 3.

Weintraub et al. (1996) obtained diffraction limited images of the L 1287 core at 3.8  $\mu\text{m}$ . In addition to RNO 1B/1C they identified at least six other stellar sources, as well as one region of nebulosity. Their image revealed a 3.8  $\mu\text{m}$  source coincident with IRAS 00338+6312, thus confirm that the outflow source is a deeply embedded protostellar object. The 3.8  $\mu\text{m}$  sources identified by Weintraub et al. (1996) are listed in Table 8.

Testi et al. (1998) included RNO 1B in their search for compact clusters around Herbig Be stars. The star is surrounded by a bright extended nebulosity. A small group

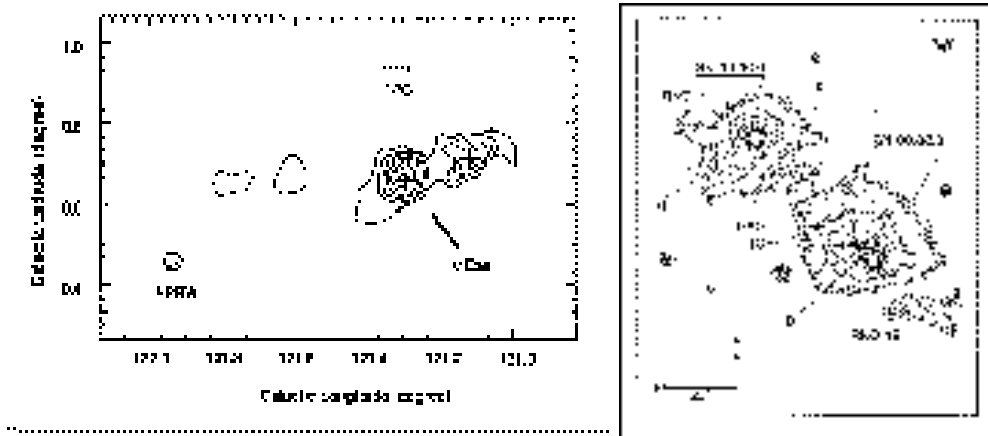


Figure 7. *Left:*  $^{13}\text{CO}$  integrated intensity map of L 1287, observed by Yang et al. (1991). Contours start at  $1 \text{ K km s}^{-1}$  with steps of  $1 \text{ K km s}^{-1}$ . IRAS 00338+6312 is denoted by cross near the center of the main peak. The cross at the west peak represents another source, IRAS 00332+6315. The direction of  $\kappa$  Cas, the assumed source of triggered formation of the dense core, is illustrated by the arrow. *Right:* I-band image of the RNO 1 region (Staude & Neckel 1991)

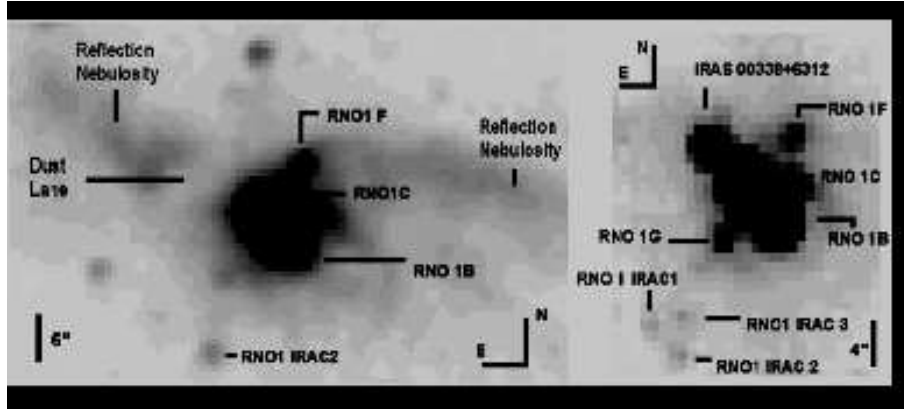


Figure 8. *Left:* The RNO 1B/1C region in the 2MASS  $K_s$  band. *Right:* The same region in the Spitzer IRAC  $5.8 \mu\text{m}$  band. Adopted from Quanz et al. (2007).

Table 8. Positions of  $3.8 \mu\text{m}$  sources in the L 1287 core (Weintraub et al. 1996)

Source	Offset RA(")	Offset Dec(")	Dist.(")
Sources Near IRAS 00338+6312			
Northern centroid	−1.50	−0.50	1.58
VLA 3	−1.20	0.20	1.22
H <sub>2</sub> O maser	−1.09	0.10	1.09
DLIRIM No. 4	−0.78	0.50	0.93
IRAS 00338+6312	0.00	0.00	0.00
DLIRIM No. 1	1.40	0.68	1.57
Other Sources			
RNO 1F	−9.60	3.09	10.39
RNO 1B	−8.10	−8.00	11.38
RNO 1D	−3.92	−6.14	7.28
RNO 1C	−3.88	−3.52	5.24
VLA 4	−0.96	−8.40	8.45
DLIRIM No. 3	−0.73	−10.62	10.65
Southern centroid	−0.15	−6.00	6.00
DLIRIM No. 2	0.18	5.12	5.12

Table 9. Positions and apparent brightnesses of IRAC sources in the L 1287 core (Quanz et al. 2007)

No.	Object name	RA(J2000)	Dec(J2000)	$3.6 \mu\text{m}$ [mag]	$4.5 \mu\text{m}$ [mag]	$5.8 \mu\text{m}$ [mag]	$8.0 \mu\text{m}$ [mag]
1	RNO 1B	00 36 46.05	+63 28 53.3	7.16	6.67	5.76	5.01
2	RNO 1C	00 36 46.65	+63 28 57.9	6.56	6.04	5.58	4.61
3	RNO 1F	00 36 45.74	+63 29 04.1	10.28	9.46	8.58	8.20
4	RNO 1G	00 36 47.14	+63 28 49.9	...	10.33	8.74	8.05
5	IRAS 00338+6312	00 36 47.34	+6 29 01.6	...	9.05	7.19	6.72
6	RNO1 IRAC1	00 36 48.44	+63 28 40.0	13.72	11.82	10.93	9.65
7	RNO1 IRAC2	00 36 47.90	+63 28 36.3	12.00	10.86	10.86	9.82
8	RNO1 IRAC3	00 36 47.85	+63 28 41.2	13.07	11.78	10.74	9.74

Table 10. IRAS point sources projected on L 1293

IRAS	F <sub>12</sub> (Jy)	F <sub>25</sub> (Jy)	F <sub>60</sub> (Jy)	F <sub>100</sub> (Jy)	L <sub>IRAS</sub> <sup>*</sup> (L <sub>☉</sub> )	Associated object
00353+6249	0.9	2.2	6.0	16.2	19	2MASS J00381870+6306053
00364+6246	1.5	0.4	<0.4	4.6	<9	HD 3572 (Sp.= K7 III)
00376+6248	<0.3	0.4	9.9	26.9	<21	

\* Assuming a distance of 850 pc.

of stars with  $r \sim 0.15$  pc was detected within the nebula. The surface density of field stars appears to increase away from RNO 1B, suggesting that localized extinction is present. The size of the cluster appears to be consistent with that of the ammonia clump detected by Estalella et al. (1993). Lorenzetti et al. (2000) present results of far-infrared spectroscopic observations, performed with ISO Long Wavelength Spectrograph, for RNO 1B.

Quanz et al. (2007) presented results of Spitzer IRAC and IRS observations of L 1287. IRAC images of L 1287 have revealed deeply embedded objects in the vicinity of RNO 1B and RNO 1C, confirming their association with a young stellar cluster. Eight sources have been detected in at least three of the four mid-infrared bands. RNO 1B/RNO 1C are the only confirmed FUors that belong to a cluster-like environment. The IRAC images resolve the mid-infrared source associated with IRAS 00338+6312, which is an intermediate-mass protostar. IRS spectra of the objects reveal their icy and dusty circumstellar environment, as well as detect H<sub>2</sub> emission lines from purely rotational transitions. These lines arise from shocked material within the molecular outflow. Table 9 lists the coordinates of objects revealed by the IRAC images (Quanz et al. 2007). The 2MASS K<sub>s</sub> and IRAC 5.8  $\mu$ m images of the L 1287 main core, adopted from Quanz et al. (2007) and displayed in Figure 8 show several faint members of the small cluster around RNO 1B/RNO 1C.

#### 4.3. L 1293

L 1293 appears as a dark cloud of opacity class 4 in Lynds' (1962) catalog. The three IRAS sources with non-stellar flux density distribution, projected on the cloud, are listed in Table 10. Whereas IRAS 00364+6246 is probably a foreground star, the two other sources may be young stellar objects associated with L 1293.

A comprehensive study of L 1293 is presented by Yang (1990). Molecular line emission was detected at  $v_{\text{LSR}} = -18 \text{ km s}^{-1}$ , close to those of the neighboring L 1287 and M 120.1+3.0, associated with Cep OB 4, suggesting that these clouds are parts of the same molecular gas stream at the same distance. Therefore Yang (1990) assumes a distance of 850 pc for L 1293. The distribution of the <sup>13</sup>CO emission is shown in the left panel of Fig. 9. The whole cloud, defined by the 2 K km s<sup>-1</sup> contour in <sup>13</sup>CO, extends over 36'  $\times$  20' or 9  $\times$  5 pc. The total mass of the cloud was estimated to be about 640 M<sub>☉</sub>. In the direction of IRAS 00376+6248 a bipolar molecular outflow was detected. A contour map of the <sup>12</sup>CO intensity for the high-velocity gas components is shown in the right panel of Fig. 9. High-resolution observations in the HCN and HCO<sup>+</sup> lines reveal a high-density region around IRAS 00376+6248.

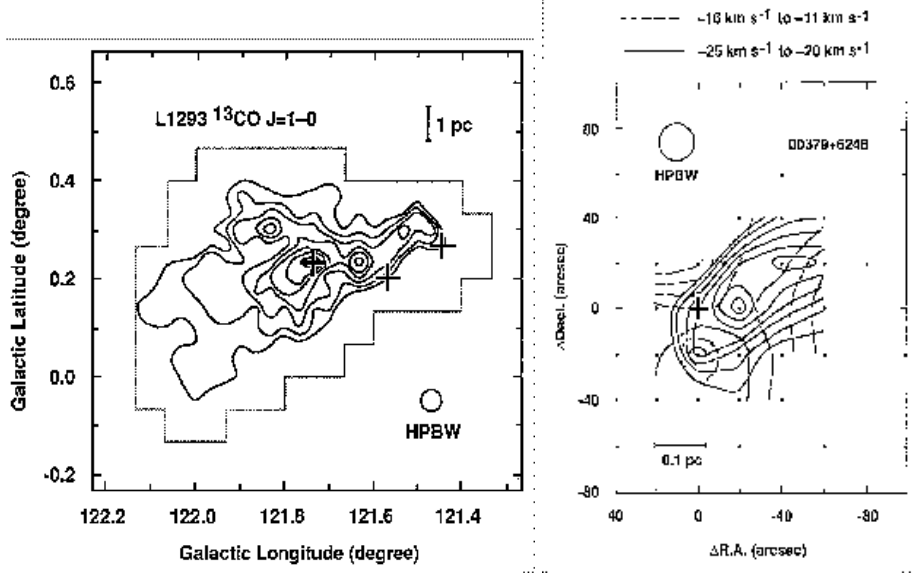


Figure 9. *Left:*  $^{13}\text{CO}$  integrated intensity map of L1293, observed by Yang (1990). Contours start at  $2 \text{ K km s}^{-1}$  with steps of  $1 \text{ K km s}^{-1}$ . The IRAS sources listed in Table 10 are plotted by crosses. *Right:* A contour map of the  $^{12}\text{CO}$  intensity for the high-velocity gas components. The solid lines and the grey lines denote the blue-shifted ( $-25 \text{ km s}^{-1} < v_{\text{LSR}} < -20 \text{ km s}^{-1}$ ) and the red-shifted ( $-16 \text{ km s}^{-1} < v_{\text{LSR}} < -11 \text{ km s}^{-1}$ ) components, respectively. IRAS 00376+6248 is indicated by a cross. (Adopted from Yang (1990).)

IRAS 00376+6248 appears in the CO survey by Wouterloot & Brand (1989) as WB 357. It is also included in the catalog of IRAS sources associated with CO gas in the outer Galaxy by Kerton & Brunt (2003) as IRCO 2387. Wouterloot et al. (1993) detected an  $\text{H}_2\text{O}$  maser emission in the direction of IRAS 00376+6248.

Olano et al. (2006) found that the space distribution and kinematics of the interstellar matter in the region of Cep OB4 suggest the presence of a big expanding shell, centered on (l,b)  $\sim (122^\circ, +10^\circ)$ . Assuming a distance of 800 pc for the center of the shell they derived a radius of some 100 pc, expansion velocity of  $4 \text{ km s}^{-1}$ , and HI mass of  $9.9 \times 10^4 M_\odot$  for the Cepheus OB4 Shell. Both L 1287 and L 1293 lie close to the low-latitude boundary of the Cep OB4 Shell, plotted in Fig. 1.

#### 4.4. Cas OB 14

L 1287 and L 1293 are located in a volume where the association Cas OB 14, defined by four high-luminosity stars, can be found (Humphreys 1978). Table 11 lists the spectral types, Galactic coordinates and absolute magnitudes  $M_V$  of these association members. The distance of 1100 pc, given by Humphreys (1978) for Cas OB 14, is the average distance of these four stars. No lower luminosity members can be found in the literature. Snell et al. (1990) and Yang et al. (1991) associate L 1287 with Cas OB 14, and propose that star formation in L 1287 might have been triggered by the strong stellar winds from  $\kappa$  Cas, the most luminous member of Cas OB 14 (see Fig. 7). As an evidence of such a trigger, Yang et al. (1991) mention that the ratio of the luminosity of the young stellar object to the mass of the core associated with the object is much higher for



the L 1287 main core than for isolated low-mass cores. Yang et al. (1991) propose that L 1287, L 1293, and M 120.1+3.0 may be parts of a giant, filamentary molecular system stretching from Cep OB 4 to Cas OB 14.

Table 11. Members of Cas OB14 (Humphreys 1978)

Star	Spectral type	$l/b$	$M_V$
HD 2905, $\kappa$ Cas	B1 Iae	120.8 / +0.1	-7.1
HD 3283	A3 Ib	121.1 / -2.5	-5.0
BD +63°48	B1 IIIne	120.3 / +1.7	-4.5
HD 2619	B0.5 III	120.7 / +2.5	-4.4

#### 4.5. BD +61°154 and its Environment (L 1302)

The pre-main sequence nature of the B8-type star BD +61°154 (MWC 419, V594 Cas) was suggested by Herbig (1960). The same paper reported on the discovery of seven H $\alpha$  emission stars, namely LkH $\alpha$  199–LkH $\alpha$  205 within 22' of BD +61°154. Five of them have HBC identifications (see Table 6). García-Lario et al. (1997) report on two further T Tauri stars in the neighborhood of BD +61°154. Testi et al. (1998) detected no density enhancement of K-band sources around this star during their infrared search for clusterings around Herbig Ae/Be stars. As BD +61°154 lies on the north-western edge of the sparse cluster NGC 225, Herbig (1960) and several other authors (e.g. Finkenzeller & Mundt 1984; Testi et al. 1998) propose that it may be a cluster member, which would suggest a distance of 650 pc (Hagen 1970). However, according to the photometric and proper motion study by Lattanzi et al. (1991) the age of NGC 225 is about 120 million years, and BD +61°154 is not a member of the cluster. Its Hipparcos parallax,  $\pi = 3.3 \pm 1.6$  (Van den Ancker et al. 1998) suggests a smaller distance. Recently, Subramaniam et al. (2006) pointed out that 15 of the 28 members of NGC 225, identified by Lattanzi et al. (1991) exhibit near-infrared excess, suggesting that the cluster is probably very young and thus may contain pre-main sequence stars.

Van den Ancker et al. (1998) associate BD +61°154 with the dark cloud L 1302. As this region lies in the Galactic plane, several clouds along the line of sight may contribute to the total extinction defining L 1302. Molecular observations confirm this hypothesis. Yang (1990) detected a weak CO emission from the direction of L 1302 at  $v_{\text{LSR}} \approx -18 \text{ km s}^{-1}$ , therefore he assumed that L 1302 belongs to the same group of molecular clouds as L 1287 and L 1293. However, other CO observations in this region report on molecular emission at  $v_{\text{LSR}} \approx -13 \text{ km s}^{-1}$  (e.g. Yonekura et al. 1997; Kerton & Brunt 2003). Kerton & Brunt (2003) detected CO emission at  $v_{\text{LSR}} = +4.41 \text{ km s}^{-1}$  and  $v_{\text{LSR}} = -13.83 \text{ km s}^{-1}$  on the position of BD +61°154 (IRCO 2414). Yonekura et al. (1997) associate their cloud 122.0 – 01.1 with L 1302 and with HBC 7 (LkH $\alpha$ 201). LkH $\alpha$ 201 appears more distant than BD +61°154 (e.g. Herbig & Bell 1988; Hernández et al. 2004). Its pre-main sequence nature is somewhat uncertain (Herbig & Bell 1988; Thé et al. 1994). Thus the distance of this system and the association of pre-main sequence stars with both each other and the clouds need further studies.

#### 4.6. S 187 and its Environment (L 1317)

S 187 is a small optical HII region (diameter:  $0''.9$ ), located in the Orion arm of the Galaxy, in the direction of the dark cloud L 1317. Its kinematic distance is  $\sim 1$  kpc. No other distance information was available in the literature until 2007, when a spectro-photometric distance of  $1.44 \pm 0.26$  kpc was published by Russeil, Adami, & Georgelin (2007). They carried out spectroscopic and photometric observation of candidate exciting stars of several HII regions, including S 187, with the aim to determine their distances. The result is based on spectral type and UBV photometric data of a B2.5V type star, located at RA(2000)= $01^h 23^m 07^s.3$ , D(2000)= $+61^\circ 51' 53''.2$  (identical with 2MASS J01230704+6151527).

S 187 belongs to a large molecular complex, mapped by Casoli, Combes, & Gérin (1984a) and Joncas, Durand, & Roger (1992). A high velocity molecular outflow was discovered by Bally & Lada (1983) near the core of the molecular cloud. The source of the outflow, S 187 IRS is close to the IRAS point source IRAS 01202+6133.

A comprehensive multi-wavelength study of S 187 can be found in Joncas et al. (1992). They mapped the ionized, neutral and molecular components of the gas complex, studied the infrared properties of the associated dust, identified IRAS point sources related to star formation, and found the possible source of the ionization by optical photometric survey of the region. (We note that their suspected exciting source (star 4) is identical with that used for distance determination by Russeil et al. (2007)). S 187 is surrounded by an HI shell and a large molecular cloud. Yonekura et al. (1997) derived  $M = 7600 M_\odot$  for the mass of the whole molecular cloud associated with S 187.

Several signposts of star formation lie in the direction of S 187, such as the IRAS source IRAS 01202+6133  $3'$  southeast of the HII region, and the outflow source S 187 IRS (Bally & Lada 1983) some  $2'$  west of the IRAS source. Henkel, Güsten & Haschick (1986) discovered  $H_2O$  maser emission from the direction of S 187 IRS. IRAS 01202+6133 is surrounded by an infrared nebula referred to as S187 IR (Hodapp 1994). Zavagno, Deharveng, & Caplan (1994) discovered an optically visible young stellar object, S187 H $\alpha$ . The optical spectrum of this object exhibits several emission lines with P Cygni type profiles. It is probably a Herbig Ae/Be star.

The left panel of Fig. 10 shows the large-scale distribution of the molecular gas overlaid on the DSS image of the field (Joncas et al. 1992). The right panel shows the map of CO outflow observed by Casoli, Combes, & Gérin (1984b), superimposed on  $V$  frames of the S 187 field obtained by Zavagno et al. (1994). The pre-main sequence star S 187 H $\alpha$  is indicated. Ammonia emission observed by Torrelles et al. (1986) is shown by thick lines.

Salas, Cruz-Gonzalez, & Porras (1998) imaged in the near-infrared a  $3''.67 \times 3''.67$  region (corresponding to  $1.07 \times 1.07$  pc<sup>2</sup>), around IRAS 01202+6133. They discovered a curved molecular hydrogen outflow that extends over a region of  $76''$  ( $0.38$  pc at  $d=1$  kpc), and identified as S187:SCP 1 (H<sub>2</sub>). The outflow changes direction by more than  $90^\circ$  in a continuous way (see the left panel of Fig. 11). The outflow-driving source is probably an extreme T Tauri star, identified as S 187 NIRS 1, located at the apex of the curved structure (identical with 2MASS J01231828+6147388). Salas et al. (1998) detected more than a hundred stars in the field. They associate the IRAS point source 01202+6133 with the reddest source in the field, with  $K = 11.7$  and  $(H - K) = 4.33$  mag (not detected in J) at the position RA(1950)= $01^h 20^m 16^s.1$  and Dec(1950)= $+61^\circ 33' 9''.8$ , (identical with 2MASS J01233317+6148482) which lies

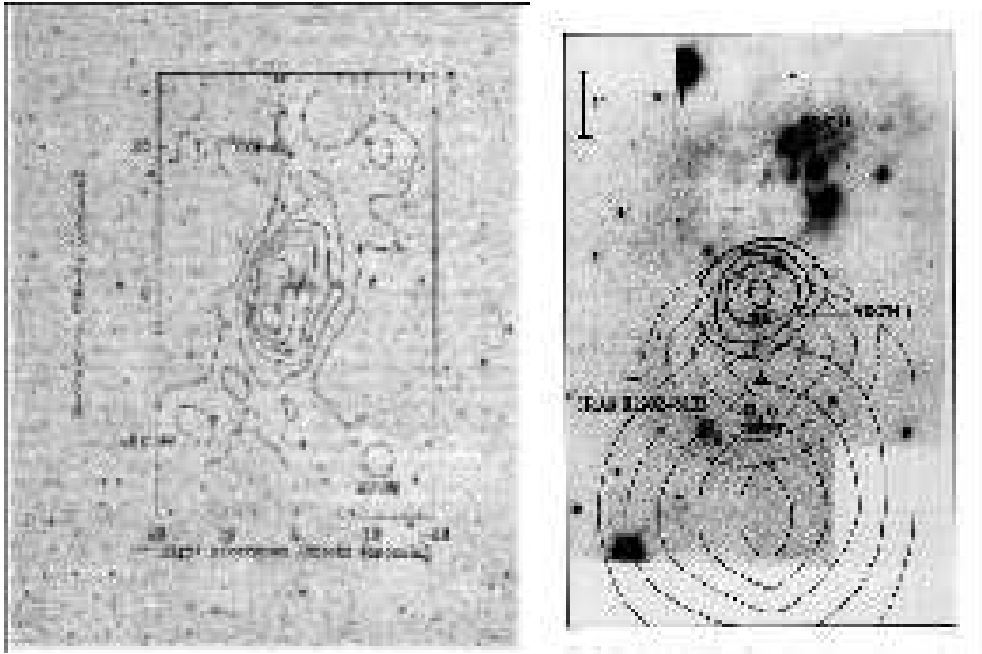


Figure 10. *Left:*  $^{13}\text{CO}$  integrated intensity map of the S 187 molecular cloud, superimposed on the Palomar Sky Survey image of the field (Joncas et al. 1992). The lowest contour and contour interval are  $2.5 \text{ K km s}^{-1}$ . The reference position is at  $01^{\text{h}}19^{\text{m}}48^{\text{s}}, +61^{\circ}35'$  (1950). The nonstellar IRAS point sources are indicated by numbers. *Right:* Map of the CO outflow observed by Casoli et al. (1984b) (dashed line for the blue wing, thin lines for the red wing), superimposed on  $V$  frames of the S 187 field obtained by Zavagno et al. (1994). Ammonia emission observed by Torrelles et al. (1986) is drawn by thick lines.

within  $13''$  of the IRAS position. This object could be a protostar or a highly extincted intermediate-mass star ( $L < 2800 L_{\odot}$ ).

Jiang et al. (2001) present  $K'$ -band polarimetric images of S 187 IR. They detected a bipolar, near-infrared nebula around IRAS 01202+6133, with the southern part being bright and knotty, and the northern part being faint and filamentary. The IRAS source 01202+6133 is located at the center of the nebula and is associated with the reddest point source of the field, labeled S1. The  $K'$ -band image is shown in the right panel of Fig. 11. The polarization map of S 187 IR reveals that the bipolar nebula is illuminated by a single central source. Bica et al. (2003) discovered an infrared cluster at  $l = 126^{\circ}66, b = -0^{\circ}79$ , associated with S 187, using the data in the 2MASS All Sky Catalog (object No. 52). S 187 has been included in the HCN ( $J=1-0$ ) survey of bright infrared sources by Pirogov (1999) and in the  $\text{N}_2\text{H}^+(1-0)$  survey of massive molecular cloud cores by Pirogov et al. (2003).

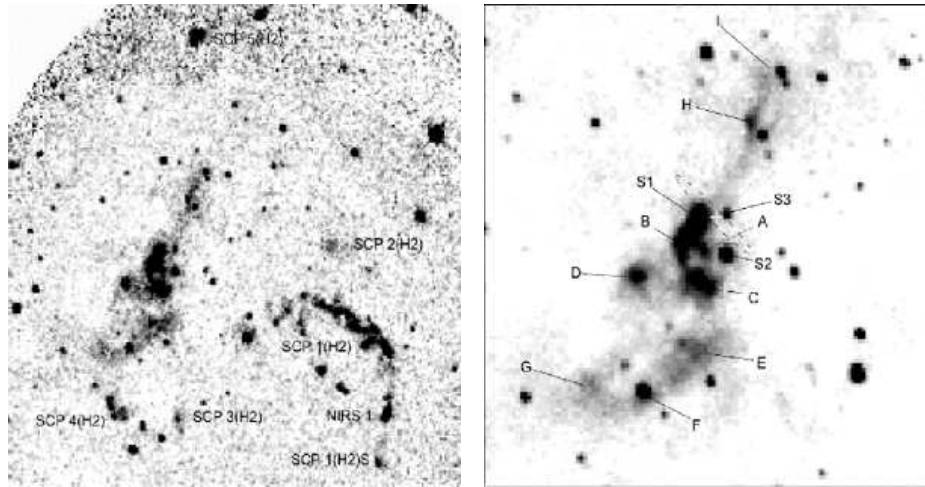


Figure 11. *Left:*  $H_2$  ( $2.122 \mu\text{m}$ ) image of S187 IR in a field of  $3'.5 \times 3'.5$  (Fig. 1 of Jiang et al. (2001)). The  $H_2$  knots detected by Salas et al. (1998) are labeled. A new  $H_2$  knot in the southwestern corner of the frame is labeled as SCP 1 (H2)S. The curved  $H_2$  jet, SCP 1 (H2), is significant to the southwest of the S187 IR nebula, and three other  $H_2$  knots are found to the north and south, generally along the nebular extension. North is up, and east is to the left. *Right:*  $K'$  image of the bipolar infrared nebula S187 IR, observed by Jiang et al. (2001). The associated NIR point sources (S1–S3) and reflection knots (A–I) are labeled. The dashed ellipse indicates the uncertainty ellipse around the position of IRAS 01202+6133.

## 5. Star Forming Regions beyond 2 kpc

### 5.1. MWC 1080: Star formation in L 1238

In spite of its large distance from the Sun, MWC 1080 (V628 Cas, HBC 317) is among the most thoroughly studied Herbig Be stars. MWC 1080 was already proposed as a candidate early-type pre-main sequence star by Herbig (1960). It is embedded in the dark cloud L 1238 at a distance of 2.2–2.5 kpc (Cantó et al. 1984; Levreault 1988). The spectral type, determined from the strength of the HeI lines by Cohen & Kuhl (1979), is B0. From a low dispersion optical spectrogram Yoshida et al. (1992) obtained A0–A3. Hernández et al. (2004) classified MWC 1080 as a continuum star. The object is a hierarchical multiple system: the primary, which is itself an eclipsing binary (Grankin et al. 1992; Leinert et al. 1997) has an infrared companion separated by  $0''.75$  (Leinert et al. 1997) and another companion at  $4''.7$  (e.g. Pirzkal et al. 1997). Zinnecker & Preibisch (1994) detected strong X-ray emission from the object. The whole system is surrounded by a small cluster of infrared sources within a radius of 0.7 pc (Testi et al. 1998). Cantó et al. (1984) discovered a CO outflow from MWC 1080. Manset & Bastien (2001) detected periodic polarimetric variations of MWC 1080 at  $7660 \text{ \AA}$ .

Hillenbrand et al. (1992) classified MWC 1080 on the basis of the shape of the SED into group I of the Herbig Ae/Be stars. The SED of this group can be interpreted by a reprocessing circumstellar disk (i.e. no accretion luminosity is required) with a central hole.

Poetzel, Mundt, & Ray (1992) reported the discovery of Herbig-Haro outflow, HH 170, associated with MWC 1080. The HH emission was found to be predominantly east of

the star, and a rather poorly collimated flow is indicated. Long-slit spectroscopy of the HH objects has shown that the radial velocities of the outflow are very high, reaching a maximum value of 400 km/s in the line wings.

Yoshida et al. (1991, 1992) studied the optical spectrum of MWC 1080, and mapped its nearby nebulosity and the surrounding molecular cloud in several molecular lines. They classified the spectral type as early A with a luminosity class of Ib-II. They found prominent P Cygni profiles in the Balmer lines up to H $\epsilon$ .

Ábrahám et al. (2000) observed MWC 1080 at mid- and far-infrared wavelengths with ISOPHOT, the photometer on-board the *Infrared Space Observatory*. They established that MWC 1080 has a peculiar SED, different from any other Herbig Be stars. With a steep flux density increase below 3.6  $\mu\text{m}$ , the ISOPHOT and ground-based data outline a plateau in  $F_\nu$  between 3.6 and 15  $\mu\text{m}$ . Around 18  $\mu\text{m}$ , however, the spectrum starts a second steep increase which culminates in a well-defined peak at 100  $\mu\text{m}$ .

The environment of MWC 1080 was resolved by KAO at 100  $\mu\text{m}$ . Di Francesco et al. (1994) derived an apparent size of 29". The presence of an extended component is also inferred from the submm observations of Mannings (1994), who measured 350 and 450  $\mu\text{m}$  flux densities in excess to the prediction of a simple optically thick accretion disk model. The source is also extended at 1.3 mm. Near-IR interferometric measurements at 2.2  $\mu\text{m}$  resolved the inner ( $r \lesssim 5''$ ) disk region of MWC 1080 (Eisner et al. 2003, 2004). Testi et al. (1998) detected a conspicuous group of stars embedded in a diffuse nebulosity around MWC 1080. The radius of the group is about 0.7 pc.

Wang et al. (2007) present CS J=2-1,  $^{13}\text{CO}$  J=1-0, and C $^{18}\text{O}$  J=1-0, observations with the 10-element BIMA array toward the young cluster around MWC 1080. These observations reveal a biconical outflow cavity with size  $\sim 0.3$  and 0.05 pc for the semi-major and semiminor axis and  $\sim 45^\circ$  position angle. These transitions trace the dense gas, which is likely the swept-up gas of the outflow cavity, rather than the remaining natal gas or the outflow gas. 32 clumps are identified in the dense gas. The clumps are approximately gravitationally bound, which suggests that they are likely collapsing protostellar cores.

## 5.2. The OB Associations in Cassiopeia

Table 12. OB associations in Cassiopeia

Name	$l_{min}$	$l_{max}$	$b_{min}$	$b_{max}$	d (kpc)	Number of massive stars		
						O type	B type	A type
Cas OB 2	110.1	114.0	-1.3	1.8	2630	2	12	2
Cas OB 5	114.9	118.0	-2.4	1.3	2500	5	10	2
Cas OB 4	119.0	121.6	-2.1	2.0	2280	5	12	...
Cas OB 14	119.7	121.1	-1.3	2.5	1100	...	3	1
Cas OB 7	121.7	125.2	-0.9	2.6	2500	1	14	1
Cas OB 1	122.3	125.8	-2.3	-0.4	2500	...	5	...
Cas OB 8	129.2	129.7	-1.5	-0.2	2900	1	10	3
Cas OB 6	133.8	138.0	-0.3	3.0	2190	17	8	...

A comprehensive study of the most luminous members of OB associations of the Cassiopeia region beyond 2 kpc has been published by Humphreys (1978). Further results on membership and Hertzsprung–Russell diagrams can be found in Garmany & Stencel

(1992). The basic data of the OB associations, taken from Humphreys (1978), are shown in Table 12. All of them, except Cas OB 14, are located in the Perseus spiral arm. The interactions of the high luminosity association members with their environments are reflected by the giant far infrared loops, discovered in the IRAS images around Cas OB 1, Cas OB 5, Cas OB 6, Cas OB 7, and Cas OB 8 by Kiss, Moór, & Tóth (2004). The shell around Cas OB 5 has been studied in detail by Moór & Kiss (2003).

**Acknowledgments.** This work was supported by the Hungarian OTKA grant T049082. I am grateful to JoAnn O’Linger for sending her results on L 1340 B before publication, and to László Szabados for careful reading of the manuscript. I used the *Simbad* and *ADS* data bases throughout this work. Comments by the referee, Yoshinori Yonekura, are greatly appreciated.

## References

- Ábrahám, P., Leinert, C., Burkert, A., Henning, T., & Lemke, D. 2000, *A&A*, 354, 965
- Anglada, G., Rodríguez, L. F., Girart, J. M., Estalella, R., & Torrelles, J. M. 1994, *ApJ*, 420, L91
- Aspin, C. & Reipurth, B. 2000, *MNRAS*, 311, 522
- Bally, J. & Lada, C. J. 1983, *ApJ*, 265, 824
- Bica, E., Dutra, C. M., Soares, J., & Barbuy, B. 2003, *A&A*, 404, 223
- Butner, H. M. & Natta, A. 1995, *ApJ*, 440, 874
- Cantó, J., Rodríguez, L. F., Calvet, N., & Lebreault, M. 1984, *ApJ*, 282, 631
- Casoli, F., Combes, F., & Gérin, M., 1984a, *A&A*, 133, 99
- Casoli, F., Combes, F., & Gérin, M., 1984b, in *Lecture Notes in Physics*, 237, *Nearby Molecular Clouds*, ed. G. Serra (Springer Verlag), p. 136
- Chavarría-K., C. 1985, *A&A*, 148, 317
- Cohen, M. 1980, *AJ*, 85, 29
- Cohen, M. & Kuhl, L. V. 1979, *ApJS*, 41, 733
- Corcoran, D., Ray, T. P., & Bastien, P. 1995, *A&A*, 293, 550
- Di Francesco, J., Evans, N. J., II, Harvey, P. M., Mundy, L. G., & Butner, H. M. 1994, *ApJ*, 432, 710
- Di Francesco, J., Evans, N. J. II, Harvey, P. M., Mundy, L. G., Guillebeau, S., & Chandler, C. J. 1997, *ApJ*, 482, 433
- Dobashi, K., Uehara, H., Kandori, R., Sakurai, T., Kaiden, M., Umemoto, T., & Sato, F. 2005, *PASJ*, 57, No. SP1
- Dorschner, J. & Gürtler, J. 1964, *AN*, 287, 257
- Eisner, J. A., Lane, B. F., Akeson, R. L., Hillenbrand, L. A., & Sargent, A. I. 2003, *ApJ*, 588, 360
- Eisner, J. A., Lane, B. F., Hillenbrand, L. A., Akeson, R. L., & Sargent, A. I. 2004, *ApJ*, 613, 1049
- Estalella, R., Mauersberger, R., Torrelles, J.M., Anglada G., Gómez, J. F., López, R., & Muders D. 1993, *ApJ*, 419, 698
- Fiebig, D. 1995, *A&A*, 298, 207
- Fiebig, D., Duschl, W. J., Menten, K. M., & Tscharnuter, W. M. 1996, *A&A*, 310, 199
- Finkenzeller, U. & Mundt, R. 1984, *A&AS*, 55, 109
- Fukagawa, M., Tamura, M., Suto, H., Itoh, Y., Murakawa, K., Oasa, Y., Hayashi, S. S., Naoi, T., Kaifu, N., & Doi, Y. 2002, *PASJ*, 54, 969
- García-Lario, P., Machado, A., Pych, W., & Pottasch, S. R. 1997, *A&AS*, 126, 479
- Garmany, C. D. & Stencel, R. E. 1992, *A&AS*, 94, 211
- Grankin, K. N., Shevchenko, V. S., Chernyshev, A. V., Ibragimov, M. A., Kondratiev, W. B., Melnikov, et al. 1992, *IBVS*, 3747
- Hagen, G. 1970, *Publ. David Dunlap Obs.*, 4, 1
- Hajjar, R. & Bastien, P. 2000, *ApJ*, 531, 494

- Henkel, C., Güsten, R., & Haschick, A. D. 1986, A&A, 165, 197
- Henning, T., Cesaroni, R., Walmsley, M., & Pfau, W. 1992, A&AS, 93, 525
- Herbig, G. H., 1960, ApJS, 4, 337
- Herbig, G. H. & Bell, K. R. 1988, Lick Obs. Bull. No. 1111 (Santa Cruz: Lick Obs.)
- Hernández, J., Calvet, N., Briceno, C., Hartmann, L., & Berlind, P. 2004, AJ, 127, 1682
- Hillenbrand, L. A., Strom, S. E., Vrba, F. J., & Keene, J. 1992, ApJ, 397, 613
- Hodapp, K. W. 1994, ApJS, 94, 615
- Humphreys, R. M. 1978, ApJS, 38, 309
- Jiang, Z., Yao, Y., Yang, J., Ishii, M., Nagata, T., Nakaya, H., & Sato, S. 2001, AJ, 122, 313
- Joncas, G., Durand, D., & Roger, R. S. 1992, ApJ, 387, 591
- Kalenskii, S. V., Promyslov, V. G., & Winnberg, A. 2007, Astron. Rep., 51, 44
- Kenyon, S.J., Hartmann, L., Gómez, M., Carr, J. S., & Tokunaga, A. 1993, AJ, 105, 1505
- Kerton, C. R., & Brunt, C. M. 2003, A&A, 399, 1083
- Kiss, Cs., Moór, A., & Tóth, L. V. 2004, A&A, 418, 131
- Koo, B. C. 1989, ApJ, 337, 318
- Kumar, M. S. N., Anandarao, B. G., & Yu, K. C. 2002, AJ, 123, 2583
- Kun, M., Nikolić, S. & Johansson, L. E. B., Balog, Z., & Gáspár, A. 2006, MNRAS, 371, 732
- Kun, M., Obayashi, A., Sato, F., Yonekura, Y., Fukui, Y., Balázs, L. G., et al. 1994, A&A, 292, 249
- Kun, M., Wouterloot, J. G. A., & Tóth, L. V. 2003, A&A, 398, 169
- Lagage, P. O., Olofsson, G., Cabrit, S., Cesarsky, C., Nordh, L., & Rodríguez-Espinosa, J. M. 1993, ApJ, 417, L79
- Lattanzi, M. G., Massone, G., & Munari, U. 1991, AJ, 102, 177
- Lee, C. W., Myers, P. C., & Tafalla, M. 1999, ApJ, 531, 366
- Lee, C. W., Myers, P. C., & Tafalla, M. 2001, ApJS, 136, 703
- Lee, C. W., Myers, P. C., & Plume, R. 2004, ApJS, 153, 523
- Leinert, C., Richichi, A., & Haas, M. 1997, A&A, 318, 472
- Levreault, R. M. 1988, ApJ, 330, 897
- Li, W., Evans II, N. J., Harvey, P. M., & Colomé, C. 1994, ApJ, 433, 199
- Lorenzetti, D., Giannini, T., Nisini, B., Benedettini, M., Creech-Eakman, M., et al. 2000, A&A, 357, 1035
- Lynds, B. T. 1962, ApJS, 4, 1
- Magakian, T. Yu., Movsessian, T. A., & Nikogossian, E. H. 2003, Astrophysics, 46, 1
- Mannings, V. 1994, MNRAS, 271, 587
- Manset, N., & Bastien, P. 2001, AJ, 122, 3453
- Matthews, B. C., Graham, J. R., Perrin, M. D., & Kalas, P. 2007, ApJ, 671, 483
- McGroarty, F., Ray, T. P., & Bally, J. 2004, A&A, 415, 189
- McMuldroch, S., Blake, G. A., & Sargent, A. I. 1995, AJ, 110, 354
- Mookerjee, B., Ghosh, S. K., Karnik, A. D., Rengarajan, T. N., Tandon, S. N., & Verma, R. P. 1999, ApJ, 522, 285
- Moór, A. & Kiss, Cs. 2003, Comm. Konkoly Obs. 103, Proc. of the conf.: *The Interaction of Stars with their Environment II.*, eds. Cs. Kiss, M. Kun, V. Könyves, p. 149
- Obayashi, A., Kun, M., Sato, F., Yonekura, Y., & Fukui, Y. 1998, AJ, 115, 274
- Olano, C. A., Meschin, P. I., & Niemela, V. S. 2006, MNRAS, 369, 867
- O'Linger, J., Moriarty-Schieven, G. H., & Wolf-Chase, G. A. 2007, AAS Abstract 211.7604
- Onishi, T., Kawamura, A., Abe, R., et al. 1999, PASJ, 51, 871
- Park, Y.-S., Lee, C. W., & Myers, P. C. 2004, ApJS, 152, 81
- Perrin, M. D., Graham, J. R., Kalas, P., Lloyd, J. P., Max, C. E., Gavel, D. T., Pennington, D. M., & Gates, E. L. 2004, Science, 303, 1345
- Pirogov, L. 1999, A&A, 348, 600
- Pirogov, L., Zinchenko, I., Caselli, P., Johansson, L. E. B., Myers, P. C. 2003, A&A, 405, 639
- Pirzkal, N., Spillar, E. J. & Dyck, H. M. 1997, ApJ, 481, 392
- Poetzel, R., Mundt, R., & Ray T.P. 1992, A&A, 262, 229
- Quanz, S. P., Henning, Th., Bouwman, J., Linz, H., & Lahuis, F. 2007, ApJ, 658, 487
- Russeil, D., Adami, C., & Georgelin, Y.M. 2007, A&A, 470, 161

- Salas, L., Cruz-Gonzalez, I., & Porras, A. 1998, ApJ, 500, 853
- Sandell, G. & Weintraub, D.A. 1994, A&A, 292, L1
- Sandell, G. & Weintraub, D. A. 2001, ApJS, 134, 115
- Sargent, A. I., van Duinen, R. J., Nordh, H. L., Aalders, J. W. G. 1981, A&A, 94, 377
- Shu, F. H. 1977, ApJ, 214, 488
- Slysh, V. I., Val'ts, I. E., Kalenskii, S. V., Voronkov, M. A., Palagi, F., Tofani, G., & Catarzi, M. 1999, A&AS, 134, 115
- Smith, K. W., Balega, Y. Y., Duschl, W. J., Hofmann, K.-H., Lachaume, R., Preibisch, T., Schertl, D., & Weigelt, G. 2005, A&A, 431, 307
- Snell, R. L., Dickman, R. L., & Huang, Y.-L. 1990, ApJ, 352, 139
- Subramaniam, A., Mathew, B., & Kartha, S. S. 2006, Bull. Astr. Soc. India, 34, 315
- Staude, H. J. & Neckel, Th. 1991, A&A, 244, L13
- Strom, K. M., Strom, S. E., Wolff, S., Morgan, J., & Wenz, M. 1986, ApJS, 62, 39
- Tachihara, K., Mizuno, A., & Fukui, Y. 2000, ApJ, 528, 817
- Tachihara, K., Neuhäuser, R., Kun, M., & Fukui, Y. 2005, A&A, 437, 919
- Tachihara, K., Onishi, T., Mizuno, A., & Fukui, Y. 2002, A&A, 385, 909
- Taylor, D. K., Dickman, R. L., & Scoville, N. Z. 1987, ApJ, 315, 104
- Testi, L., Palla, F., & Natta, A. 1998, A&AS, 133, 81
- Thé, P. S., de Winter, D., & Pérez, M. 1994, A&AS, 104, 315
- Torrelles, J. M., Ho, P. T. P., Moran, J. M., Rodríguez, L. F., & Cantó, J. 1986, ApJ, 307, 787
- Turner, D. G., & Evans, N. R. 1984, ApJ, 283, 254
- Van den Ancker, M. E., De Winter, D., & Tjin A Djie, H. R. E. 1998, A&A, 330, 145
- Walker, R. N. F., & Masheder, M. R. W. 1997, MNRAS, 285, 862
- Wang, S., Looney, L. W., Brandner, W., & Close, L. M. 2007, ApJ, 673, 315
- Weintraub, D. A., & Kastner, J. H. 1993, ApJ, 411, 767
- Weintraub, D. A., Kastner, J. H., Gatley, I., & Merrill, K. M. 1996, ApJ, 468, L45
- Wouterloot, J. G. A., & Brand, J. 1989, A&AS, 80, 149
- Wouterloot, J. G. A., Brand, J., & Fiegle, K. 1993, A&AS, 98, 589
- Yang, J. 1990, *A Study of Molecular Clouds and Star Formation in the Cepheus–Cassiopeia Region*, Thesis, Nagoya University
- Yang, J., Fukui, Y., Umemoto, T., Ogawa, H., & Chen, H., 1990, ApJ, 362, 538
- Yang, J., Ohashi, N., & Fukui, Y. 1995, ApJ, 455, 175
- Yang, J., Umemoto, T., Iwata, T., & Fukui, Y. 1991, ApJ, 373, 137
- Yonekura, Y., Dobashi, K., Mizuno, A., Ogawa, H., & Fukui, Y. 1997, ApJS, 110, 21
- Yoshida, S., Kogure, T., Nakano, M., Tatematsu, K., & Wiramihardja, S. D. 1991, PASJ, 43, 363
- Yoshida, S., Kogure, T., Nakano, M., Tatematsu, K., & Wiramihardja, S. D. 1992, PASJ, 44, 77
- Zavagno, A., Deharveng, L., & Caplan, J. 1994, A&A, 281, 491
- Zinnecker, H. & Preibisch, T. 1994, A&A, 292, 152